Surface Science 603 (2009) 1605–1612

Contents lists available at ScienceDirect

Surface Science

journal homepage: www.elsevier.com/locate/susc

Photochemistry on TiO_2: Mechanisms behind the surface chemistry

John T. Yates Jr. *

Department of Chemistry, University of Virginia, Charlottesville, VA 22904, USA

ARTICLE INFO

Article history:
Available online 21 January 2009

Keywords:
TiO_2
Photochemistry
Photodesorption
Oxygen
O_2
Hydrophilic
H_2O
Hydrocarbon film

ABSTRACT

Photochemistry from TiO_2 surfaces is described for two cases: The UV-induced photodesorption of O_2 from $TiO_2(110)-1\times1$; and the hydrophilic effect caused by UV irradiation on TiO_2. In both cases fundamental information about how these processes occur has been found. In the case of the O_2 photodesorption kinetics, it has been found that the rate of the process is proportional to the square root of the UV flux, showing that second-order electron–hole pair recombination is dominant in governing the photodesorption rate. In addition these measurements provide an estimate of the concentration of hole traps in the TiO_2 crystal. In other measurements of the UV-induced hydrophilicity, starting with the atomically-clean TiO_2 surface, it has been shown that the effect occurs suddenly at a critical point during irradiation as a result of photooxidation of a monolayer of hydrocarbon (*n*-hexane) at equilibrium with ppm concentration of *n*-hexane in O_2 at 1 atmosphere pressure.

1. Introduction

The winning of the Nobel Prize in Chemistry in 2007 by Gerhard Ertl represents a singular recognition of the importance of the field of surface chemistry as practiced in the latter half of the twentieth century. The Prize recognized an exciting and significant area of scientific research, as well as the work of a highly admired scientist who has led the way in the field. The majority of the work done in this period by Ertl and others [1], has dealt with the type of surface chemistry which is thermally activated, and indeed, the thermal activation of surface processes currently drives the majority of technological applications of surface chemistry.

There is another mode of surface species' activation which is driven by electronic excitation. Here, either the electronic activation of surface species, or the electronic activation of the substrate, on which the surface species reside, is the first step in causing new surface chemistry to occur [2]. The exploration of the electronic activation of surface processes now occurs at a very active research frontier and will in the future grow significantly as interest in harnessing sunlight to produce electricity and to cause new surface reactions increases. Indeed the ability to initiate surface chemistry by electronic excitation opens new vistas for research and applications which have in the past mainly been recognized by the DIET (Desorption Induced by Electronic Transitions) Conferences [3] as well as by several Surface Science Reports [4], and Chemical Reviews [2,5,6].

This short review summarizes work in the photoactivation of surface chemistry on semiconductor TiO_2 surfaces. It is partly based on earlier reviews of this topic [2,5,6] by ourselves, as well as on recent work which has been done. In 1972, Fujishima and Honda discovered the photosplitting of water on TiO_2 electrodes [7], offering the potential for $H_2(g)$ and $O_2(g)$ production from sunlight. This was followed by the development of a sunlight-driven photovoltaic cell which employs dye-modified TiO_2 electrodes, the Graetzel cell [8–10]. These two important developments were accompanied by much research and engineering in a third area, leading to the use of TiO_2 as a photochemical substrate for photooxidation reactions, a major application area. A wide range of new methods for "slow-but-sure" solar-driven environmental remediation of contamination by organic matter in the atmosphere and in water medium has resulted from this effort. Prime examples of this include self-cleaning windows coated with TiO_2 films [11] and TiO_2-based paints and films [11] which clean themselves in sunlight leaving white surfaces after extensive exposure to dirty atmospheres, followed by washing by rain. In addition, photochemically induced hydrophilicity [12] and photoinduced antimicrobial [11,13] properties of TiO_2 films have recently been discovered and these ideas are now employed for new photochemically activated cleaning technologies driven by sunlight, or even by the small ultraviolet component of fluorescent lighting inside buildings.

2. Photoexcitation on semiconductor surfaces-basic principles

Fig. 1 shows a schematic of the photoexcitation of a semiconductor solid particle by exposure to radiation with energy above the bandgap energy [5]. An exciton, produced by the absorption of a photon is shown by the star symbol. This is followed by charge separation – the production of an electron–hole pair. Charge

* Tel.: +1 434 924 7514.
E-mail address: johnt@virginia.edu

0039-6028/$ - see front matter © 2009 Elsevier B.V. All rights reserved.
doi:10.1016/j.susc.2008.11.052

Report Documentation Page

Form Approved
OMB No. 0704-0188

1. REPORT DATE	2. REPORT TYPE	3. DATES COVERED
2009		**00-00-2009 to 00-00-2009**

4. TITLE AND SUBTITLE	5a. CONTRACT NUMBER
Photochemistry on TiO2: Mechanisms behind the surface chemistry	**W911NF--4-1-0200**
	5b. GRANT NUMBER
	5c. PROGRAM ELEMENT NUMBER
6. AUTHOR(S)	5d. PROJECT NUMBER
	5e. TASK NUMBER
	5f. WORK UNIT NUMBER
7. PERFORMING ORGANIZATION NAME(S) AND ADDRESS(ES) **Department of Chemistry,University of Virginia,Charlottesville,VA,22904**	8. PERFORMING ORGANIZATION REPORT NUMBER **; 45758-CH.12**
9. SPONSORING/MONITORING AGENCY NAME(S) AND ADDRESS(ES) **U.S. Army Research Office, P.O. Box 12211, Research Triangle Park, NC, 27709-2211**	10. SPONSOR/MONITOR'S ACRONYM(S)
	11. SPONSOR/MONITOR'S REPORT NUMBER(S) **45758-CH.12**

12. DISTRIBUTION/AVAILABILITY STATEMENT
Approved for public release; distribution unlimited

13. SUPPLEMENTARY NOTES

14. ABSTRACT

15. SUBJECT TERMS

16. SECURITY CLASSIFICATION OF:			17. LIMITATION OF ABSTRACT	18. NUMBER OF PAGES	19a. NAME OF RESPONSIBLE PERSON
a. REPORT **unclassified**	b. ABSTRACT **unclassified**	c. THIS PAGE **unclassified**	**Same as Report (SAR)**	**8**	

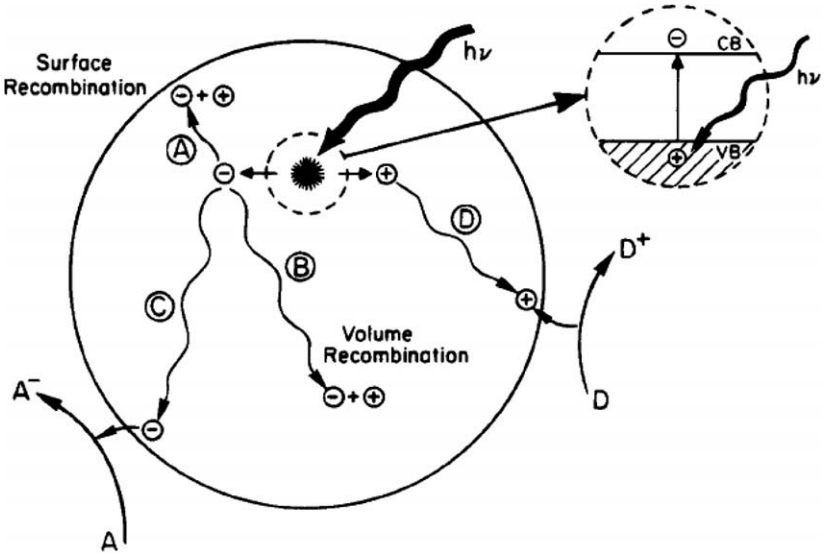

Fig. 1. Schematic photoexcitation in a semiconductor particle followed by later events [5].

transport to the particle surface by processes C and D lead respectively to desirable reduction and oxidation reactions at the surface. Processes A and B represent electron–hole pair recombination processes at the surface and in the bulk, respectively.

The quantum yield, Φ, for such a combination of processes is

$$\Phi = k_{CT}/(k_{CT} + k_R) \quad (1)$$

where k_{CT} is the rate constant for charge transfer and k_R is the rate constant for recombination. The quantum yield would approach unity if recombination processes were eliminated, but this is never the case. Indeed, the issue of recombination plagues the field of semiconductor activation by light, both in the field of surface photochemistry and in photovoltaic applications. Modifications to semiconductors by doping or by metal deposition or by combinations with other semiconductors are able to decrease the recombination rate thereby increasing the quantum yield (Ref. [5], Section 4).

Fig. 2 shows a schematic energetic picture of surface or bulk electron trap states. These states exist in crystalline and colloidal TiO_2 where surface oxygen vacancy defects and defects in the crystalline lattice provide new localized energy states not available in the perfect crystal. In addition, since the perfect surface represents an abrupt discontinuity from the lattice, it too provides a high density of energy states in the surface region. These energy states differ in their energy from the energy bands present in the perfect solid and can act as traps for electrons, enhancing the recombination process and producing shorter hole lifetimes, which is detrimental to the efficiency of surface photochemistry driven by hole production.

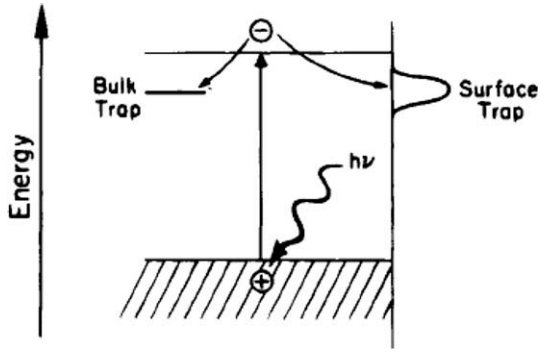

Fig. 2. Surface and bulk electron carrier trapping leading to an enhanced charge carrier recombination rate and shorter hole lifetimes [5].

Fig. 3 shows a schematic diagram after Shockley, Read and Hall [14] which shows the trapping of electrons and holes in the semiconductor. Once trapped, the hole or electron is annihilated at a rate which is faster than in the absence of trap, resulting in shorter hole lifetimes. Four indirect electronic transition processes are illustrated. Process 1 illustrates electron capture from the conduction band by a recombination center which is neutral before charge capture and which lies within the energy gap for the semiconductor. The rate of capture of the thermally excited electrons is proportional to the density of the recombination centers, and the capture cross section, which is of order of atomic dimensions, $\sim 10^{-15}$ cm^2. Process 2 illustrates the rate of emission of electrons from the recombination center; under equilibrium conditions this rate will be equal to the electron capture rate. Process 3 represents a hole capture process where a trapped electron recombines with a hole in the valence band; the rate of the process is related to the product of the trapped electron concentration and the hole concentration. Process 4 is termed hole emission and describes the excitation of an electron from the valence band to an electron trap state, leaving a hole in the valence band. When the semiconductor is illuminated the charge carrier concentration increases above that at thermal equilibrium. Processes 1 and 3 together constitute a recombination process which removes electrons and holes at the trap site, diminishing the photochemical reaction rates induced either by available holes or electrons.

3. Using surface chemical photokinetics to observe charge carrier recombination and the presence of hole traps

The photodesorption of O_2, adsorbed on TiO_2 (1 1 0), provides a relatively simple surface process with easily-measured kinetics which can be used to directly observe hole trapping by its kinetic effect. Fig. 4 shows the apparatus used in these measurements. A filtered Hg UV source, of measured intensity, emitting radiation selected within 10 nm wide spectral regions, is focused on the crystal containing adsorbed O_2, and a shutter controls the exposure to light.

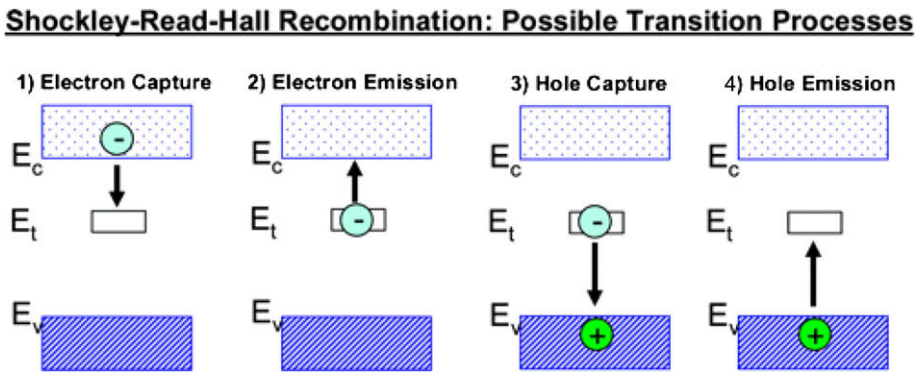

Fig. 3. Schematic of four electronic transition processes that may occur and which relate to charge carrier recombination at trap sites [6,14].

The rate of photodesorption of chemisorbed O_2 from TiO_2(1 1 0) has been studied carefully as a function of the photon energy, and typical results are shown in Fig. 5 [16]. It may been seen that the threshold for photodesorption is near the rutile TiO_2 bandgap, about 3.0 eV. Thus for this crystal, a photon energy near the bandgap energy is necessary for excitation of the O_2 desorption reaction, and the natural dopant and defect level in the crystal does not influence the threshold energy appreciably.

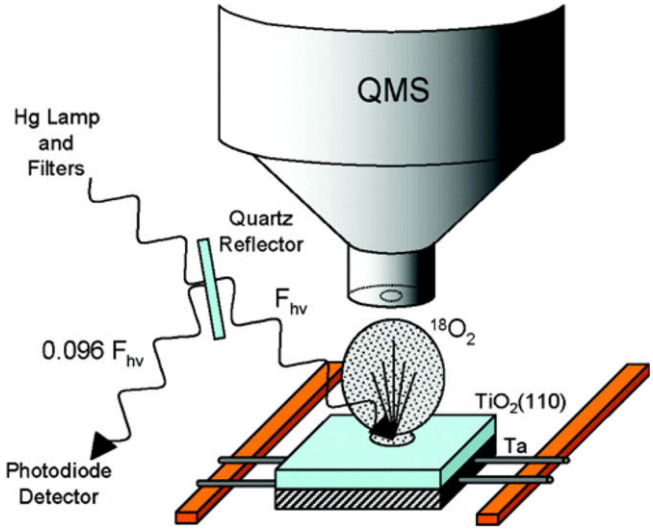

Fig. 4. Ultrahigh vacuum apparatus for the quantitative study of photodesorption from TiO_2 [15].

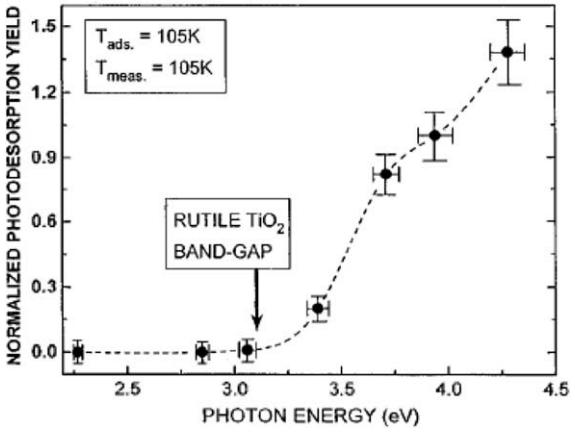

Fig. 5. Excitation of O_2 photodesorption near the bandgap energy of rutile-TiO_2(1 1 0) [16].

The chemisorbed O_2 molecules are known to be localized on O-vacancy defects on the surface and to become negatively charged upon adsorption [15,17–21]. Photodesorption is thought to be caused by photogenerated holes which interact with the adsorbed O_2 molecules [19–21]. Upon irradiation, a line-of-sight mass spectrometer detects desorbing O_2, and the intensity of the O_2 signal is a direct measure of the rate of photodesorption, $-d\theta_{O_2^-}/dt$. Using steady state kinetics in the four-step process shown in Eqs. (2)–(5), the rate of O_2 desorption is expressed in Eq. (6)

$$h\nu + TiO_2 \xrightarrow{k_1 F_{h\nu}} e^- + h^+ \tag{2}$$

$$h^+ + T \xrightarrow{k_2} T^+ \text{ (hole capture by a hole trap)} \tag{3}$$

$$e^- + h^+ \xrightarrow{k_3} \text{heat (on recombination sites)} \tag{4}$$

$$h^+ + O_2^-(a) \xrightarrow{k_4} O_2(g) \uparrow \tag{5}$$

$$-d\theta_{O_2^-}/dt = k_4\theta_{O_2} - \left[\frac{k_1}{k_3}\right]^{1/2} F_{h\nu}^{1/2} \tag{6}$$

Assuming steady state kinetics, where electron–hole recombination (Eq. (4)) is the dominant process, the overall desorption rate shown in Eq. (6) is seen to be proportional to the square root of the light flux, $F_{h\nu}^{1/2}$. This is a result of the second-order electron–hole pair recombination rate where the concentration of holes is essentially equal to the concentration of electrons. The observation of the $F_{h\nu}^{1/2}$ rate law is an indirect indication of the dominance of charge carrier recombination on the magnitude of the O_2 photodesorption process, and good measurements of the ½-power rate law for photochemical processes on surfaces have not been reported previously.

Fig. 6 shows a plot of the rate of O_2 desorption versus $F_{h\nu}^{1/2}$. It is observed that the plot consists of two linear branches, A and B. At $F_{h\nu}^{1/2}$ (crit.) a break in the two branches is observed. The position of the breakpoint is an indicator that hole trap sites in and on the crystal have been saturated by photogenerated holes at the critical light fluence in the short (0.1 s) measurement time yielding the initial rate, Y^0, of photodesorption, and that more efficient hole transfer to adsorbed O_2-species takes place at light fluxes beyond this hole-trap saturation point.

Fig. 7 shows a schematic diagram of the hole trapping process [22] coupled with the transfer of charge between the hole and the adsorbed O_2 molecule. The O_2 molecules, adsorbed at oxygen vacancy defect sites are negatively charged [15,17–21] and would

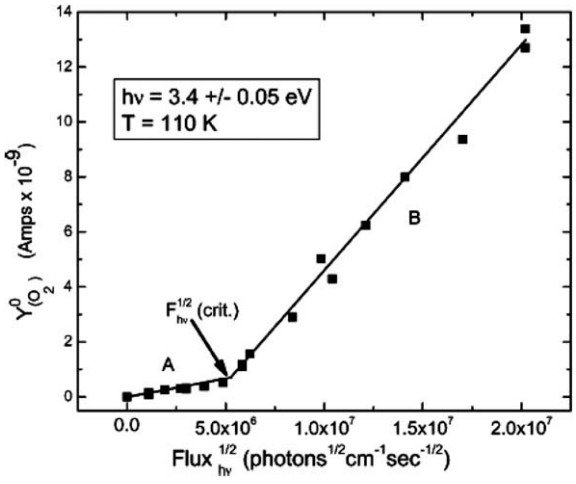

Fig. 6. Initial yield of photodesorbing O_2 for increasing photon flux. The oxygen coverage is identical for each point and the initial rate of O_2 photodesorption is measured for each point [22].

naturally donate an electron to an approaching hole. The detailed mechanism for placing the O_2 molecule on a repulsive potential curve as a result of its interaction with the hole is unknown. Experiments show that $^{18}O_2$, adsorbed at defect sites on $Ti^{16}O_2$, do not undergo isotopic exchange with the lattice and instead desorb only as $^{18}O_2$ [23]. Thus the charge transfer process causes only the rupture of the surface-O_2 bond when O_2 desorption is measured. Earlier work has shown that another channel is also photochemically excited. This second channel produces reactive oxygen species of unknown structure and stoichiometry which are able to cause photooxidation of adsorbed CO [24], and likely other oxidizable molecules.

In related work, it has been found that the photooxidation of formate ions in aqueous solution follows an $F_{hν}^{0.61}$ dependence. Recent work by Cornu et al. [25] has shown that the dynamics measured in the fast time regime (picoseconds and slightly above) are not relevant to surface photochemistry and that slower dynamics,

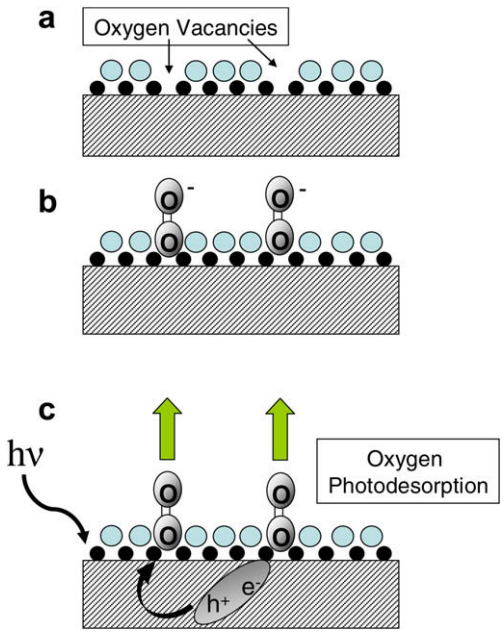

Fig. 7. Schematic of hole generation and hole trapping in connection with the excitation of O_2 photodesorption from TiO_2(110) [22].

such as those studied in our O_2/TiO_2(110) work, are dominant, with lifetimes being measured in the millisecond regime.

The work described above involving the photodesorption of O_2 has been employed to study photophysical aspects of surface chemistry using a comparatively simple system. In more complex surface photooxidation reactions, sequential excitation steps involving more than one photon and more than one charge carrier will lead to complex kinetics involving multiple intermediate oxidation products and multiple elementary steps. Kinetic studies, based on these more complex photooxidation processes are difficult to interpret, and are generally unsuitable for investigation of the basic underlying photokinetic steps involving charge transfer and reaction chemistry which are at work.

It is possible to estimate the hole-trap density from the measurements of the value of $F_{hν}$(crit.) for O_2 photodesorption [22], and the hole-trap density is found to be about 3×10^{18} cm^{-3}. The calculated hole-trap density assumes that all photons are absorbed in the first 100 Å of the surface, a penetration depth consistent with the optical absorption coefficient for TiO_2.

4. Application of surface science methods for the understanding of the mechanism of photoinduced hydrophilicity on TiO_2 surfaces

The photoinduced hydrophilic effect was first reported by Wang et al. [12] on TiO_2 films and the effect is shown in Fig. 8. UV irradiation in air causes water droplets to wet the TiO_2 film surface, resulting in a lowering of the contact angle over time.

The anatase TiO_2 film was deposited on a glass surface followed by annealing to 773 K [26]. The experiment was carried out in the ambient atmosphere, and this study and many others have shown that under these conditions, the contact angle decreases slowly during interrupted irradiation periods, as shown in Fig. 9. Both anatase and rutile films were investigated and it was concluded that the UV-induced wetting phenomenon was an inherent property of TiO_2. Wang, et al. postulated that UV light induced the formation of oxygen vacancies and that these vacancies caused the dissociation of water to form hydrophilic surface OH groups [12]. In addition in 2003, Sakai et al. [26], from the same group, postulated that UV modification of the TiO_2 surface followed by water adsorption changed the nature of OH groups' binding from twofold binding to onefold binding to Ti sites. In contrast to this report, recent infrared studies [27] carried out on high area TiO_2 containing adsorbed H_2O as well as Ti-OH groups showed that intense UV irradiation for long times in the presence of gas phase O_2 did not alter the IR spectrum, indicating that UV irradiation has no influence of the hydroxyl groups in connection with the UV-initiated hydrophilicity on TiO_2.

It is seen in Fig. 9 that measurements made in ambient air show that the UV-induced hydrophilic effect is a slow effect, occurring over many minutes in the laboratory air. Previously the same authors using similar measurement methods [12] had also proposed that photoinduced oxygen vacancy defect formation (Ti^{3+} surface ion formation) was responsible for the effect.

Using the STM, we were able to show that defect production on rutile TiO_2(110) – 1×1 surfaces could not be responsible for the hydrophilic effect [28]. Thus in Fig. 10, a partially defective surface was exposed to 5.4×10^{21} photons cm^{-2}. The photon energy was above 3.0 eV. No defect production was observed and an upper limit of the cross section for defect production was estimated to be of order $10^{-23.5}$ cm^2.

Recent theoretical work by Bouzoubaa et al. [29] has shown that defect production would require energy above the 4.5–7 eV range, depending upon the final state of the desorbing oxygen. This work therefore shows that UV irradiation at lower photon energies could

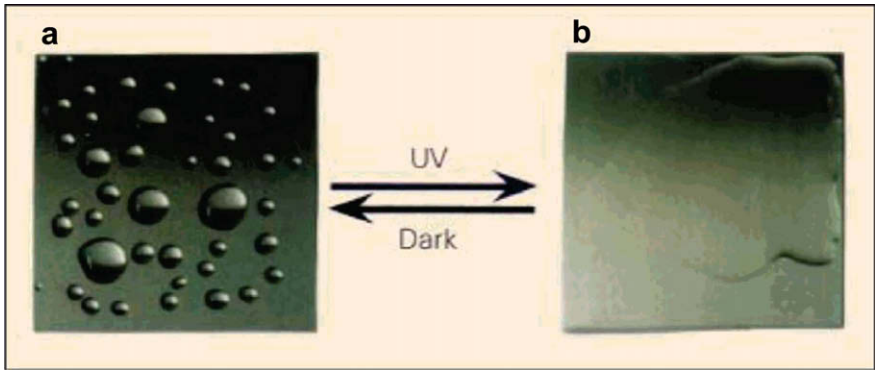

Fig. 8. Light induced wetting of a TiO_2 film in air upon exposure to UV irradiation. (a) Hydrophobic TiO_2 film with water droplets; (b) hydrophilic TiO_2 film after UV exposure [12].

not produce defect sites, in agreement with the STM experiments [28].

In contrast to the measurements of a slow change in contact angle, recent measurements in our laboratory to be described below [27] have shown that in fact, the UV generated hydrophilicity phenomenon is a sudden effect when the oxygen-containing atmosphere, containing known low level amounts of hydrocarbon, is well controlled and when the exposure to UV irradiation is continuous. In contrast, the measurements shown in Fig. 9 were made in ambient air with uncontrolled hydrocarbon content and under conditions where the exposure to UV irradiation was interrupted for contact angle measurements, during which time exposure to the uncontrolled hydrocarbon-contaminated ambient air was continued.

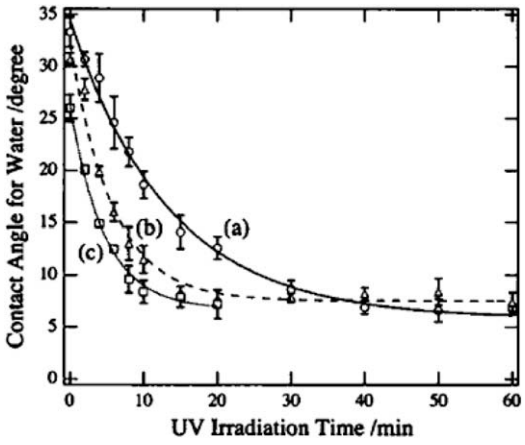

Fig. 9. Changes of the contact angle for water on a TiO_2 film following irradiation with UV light in ambient air at three light power densities. (a) 0.2 mW cm^{-2}; (b) 0.7 mW cm^{-2}; (c) 1.0 mW cm^{-2}. The irradiation was interrupted for measurement of the contact angle [26].

Fig. 11 shows the ultrahigh vacuum apparatus designed to specifically study the UV-induced hydrophilicity on an initially atomically-clean $TiO_2(110)$ – 1×1 single crystal under highly controlled surface and gas phase conditions. The crystal is studied by pure water contact angle measurements in a water-saturated oxygen atmosphere containing controlled ppm levels of *n*-hexane. In contrast to measurements made in ambient air [12,26], where hydrocarbon contamination is likely to have occurred between contact angle measurements, our measurements are made continuously.

The ultrahigh vacuum apparatus contains two chambers which may be isolated from each other either by a gate valve or by a doubly-differentially pumped sliding Teflon seal. The preparation chamber to the right is used to prepare the atomically-clean TiO_2 (110) – 1×1 single crystal and to characterize it by Auger spectroscopy and LEED. The usual cleaning method, involving Ar ion sputtering and oxygen treatment were used in crystal preparation [22]. The clean crystal was then transferred to the experimentation chamber, where a droplet of highly purified conductivity water (18.2 MΩ cm) could be added to the crystal. In control measurements, where the water droplet was evaporated and the crystal was then transferred back to the preparation chamber for Auger analysis, it was found that significant contamination by the water

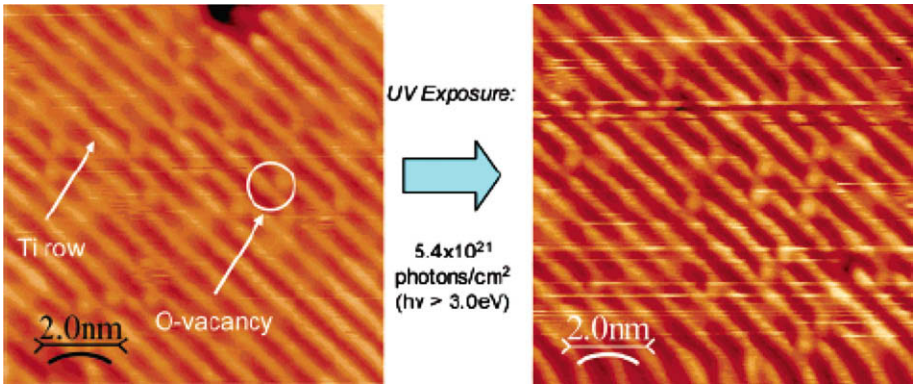

Fig. 10. STM images of the partially reduced $TiO_2(110)$ – 1×1 surface after exposure to 5.4×10^{21} UV photons cm^{-2} with $h\nu > 3.0$ eV. No additional defect formation is observed following this very high light exposure in several experiments [28].

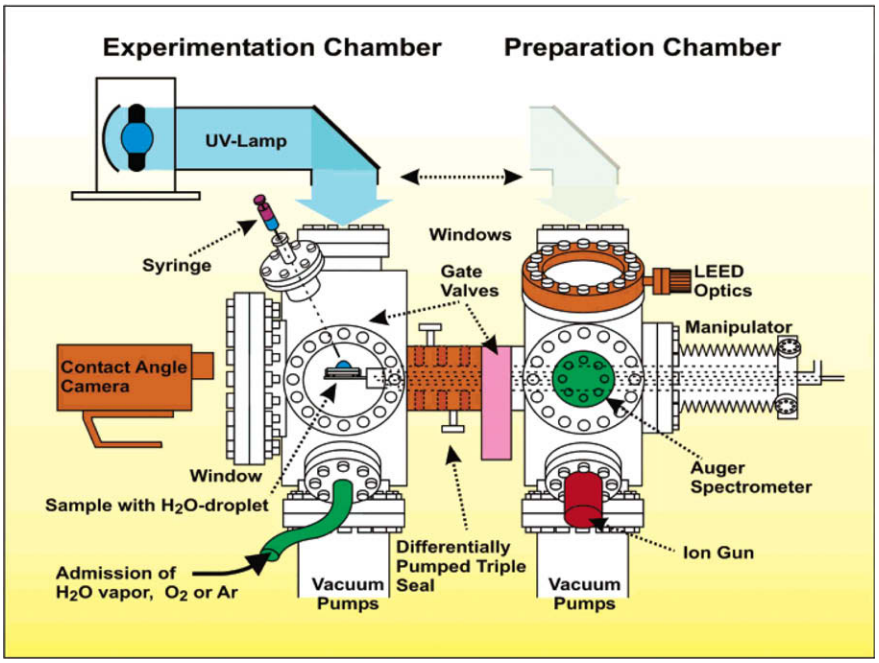

Fig. 11. Diagram of apparatus for in situ studies of the water contact angle on TiO_2(1 1 0) during UV irradiation in controlled 99.9999% pure O_2 atmosphere (<0.05 ppm background hydrocarbon) containing known ppm levels of added hydrocarbon contamination [27].

was not occurring and only about 0.05 ML of carbon was detected after evaporation of a ~2 mm diameter droplet. To achieve such low levels of contamination, a method of insertion of a syringe needle to deposit the pure water was devised, consisting of a stainless steel tube which conducts the syringe needle into the pressurized chamber to near the crystal surface; outflow of oxygen through the stainless steel insertion tube prevents atmospheric and other contamination within the chamber during water addition. Experiments performed with a rubber septum seal invariably left silicon and other contaminants on the surface after water evaporation. For the UV-induced hydrophilicity experiments, a droplet of pure water was deposited in the O_2 atmosphere which is saturated with water vapor. It was then irradiated from the UV lamp from above and the contact angle was automatically recorded as a function of time with an electronic camera.

Fig. 12 shows images of the sudden wetting of the TiO_2 surface at a critical UV exposure time of 155 s. By mathematically fitting the meniscus shape of the water droplet it is possible over the course of the experiment to measure the contact angle to 1° at high angles, but errors of <7–9° occur at the lower limit.

A number of experiments of the type shown in Fig. 12 were done at various concentrations of *n*-hexane and three representative experiments are shown on the left hand display of Fig. 13.

These experiments differ greatly from the work of others (as shown for example in Fig. 9) where a slow wetting effect is always seen. We believe that in the work of others the interruption of the irradiation experiment for the measurement of contact angle at each point is the crucial difference. During the sequence of measurements, ambient hydrocarbons are allowed to build up on the surface when contact angles are being measured and this prevents the observation of the sudden effect. It is the sudden effect which holds the clue as to the origin of the UV-induced hydrophilicity on TiO_2 when irradiated in the air.

The observation of the sudden effect whose induction time scales linearly with the concentration of added hydrocarbon suggests a simple model to explain the photoinduced hydrophilicity phenomenon. We assume that *n*-hexane establishes an equilibrium coverage on the TiO_2 surface at 300 K. Under these conditions,

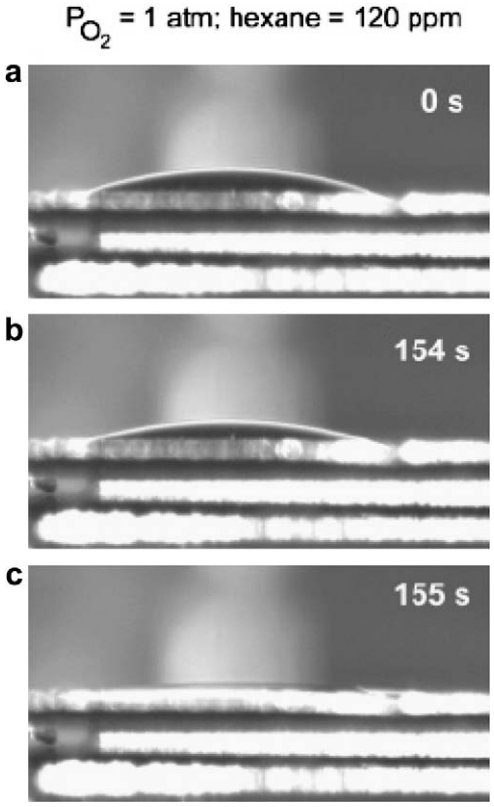

Fig. 12. (a) Water droplet on non-irradiated TiO_2 in mixed O_2 + *n*-hexane (120 ppm) atmosphere at one atmosphere total pressure; (b) the same water droplet after 154 s UV exposure; (c) sudden and complete wetting of the same droplet after 155 s exposure to UV irradiation [27].

the rate of *n*-hexane adsorption and of desorption are balanced. When photooxidation occurs the balance of adsorption/desorption rates is disturbed and a net rate of loss of *n*-hexane takes place un-

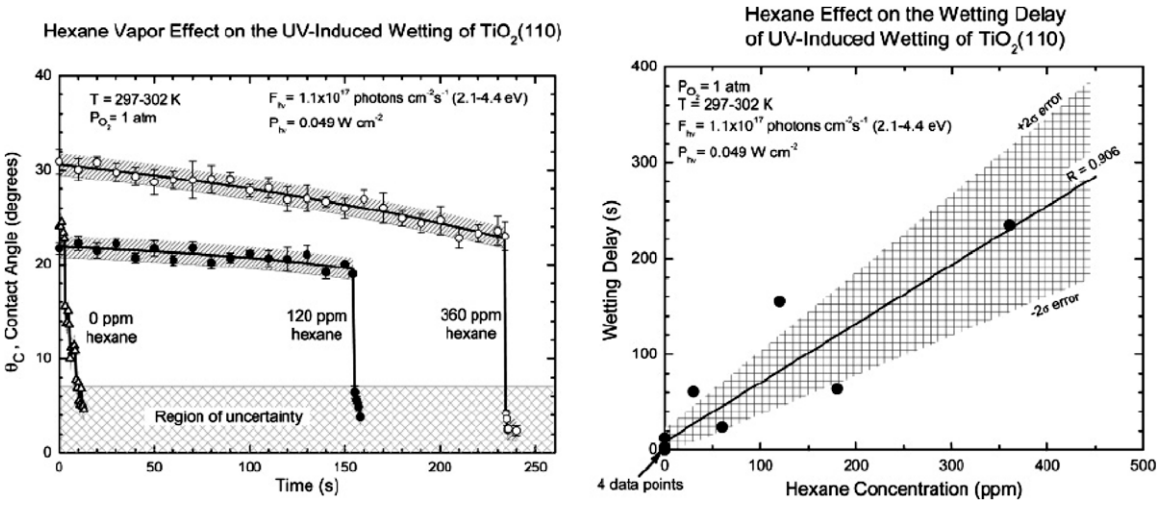

Fig. 13. Measured contact angles for water droplets on the TiO_2 surface, exposed to various levels of hexane in an O_2 atmosphere. The left hand graph shows three typical experiments where the small decrease in contact angle before the sudden effect is due to slight evaporation of the water droplet. The right hand graph shows the results of 9 experiments. Note that 4 experiments confirm the near zero contact angle achieved in only a few seconds irradiation when no added hexane was employed. The induction period for sudden wetting scales linearly with the *n*-hexane concentration in the O_2 atmosphere as shown in the right hand graph [27].

der constant UV irradiation. Thus, a continuous decrease in the hydrocarbon coverage occurs when photooxidation takes place in the hydrocarbon-containing atmosphere. The induction period scales in proportion to the rate of hydrocarbon adsorption; higher gas phase concentrations of hydrocarbon increase the time required to deplete the adsorbed hydrocarbon initially in equilibrium with the ppm hydrocarbon concentration in the gas phase. It is likely that the coverage of adsorbed hydrocarbon at the outer perimeter of the water droplet controls the wetting phenomenon. When the surface coverage of adsorbed hydrocarbon there drops to a critical low level due to photooxidation, the water droplet suddenly wets the surface. A schematic picture of this effect is shown in Fig. 14.

Fig. 15 shows a schematic of the proposed mechanism for UV-induced hydrophilicity on TiO_2. In the top of Fig. 15, a non-wetting monolayer of adsorbed hydrocarbon molecules is initially present over the entire surface as shown by thin black symbols. This layer is in equilibrium with the gas phase hydrocarbon. The rate of adsorption/desorption will increase in proportion to the hydrocarbon partial pressure up to saturation of the hydrocarbon mono-

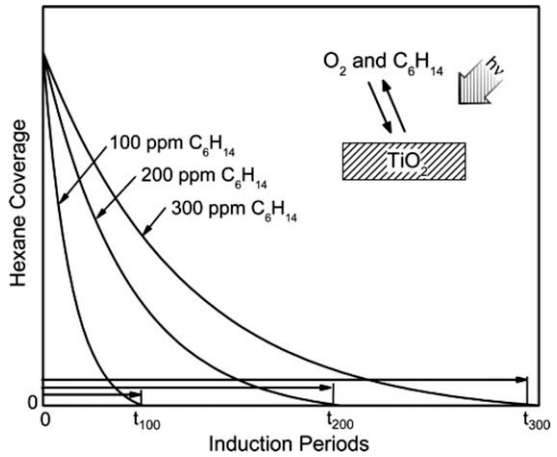

Fig. 14. Schematic model of the effect of gas phase *n*-hexane on its photooxidation kinetics, where it is assumed that all experiments begin at a saturated hexane monolayer. Increasing induction periods are indicated for increasing partial pressures of *n*-hexane [27].

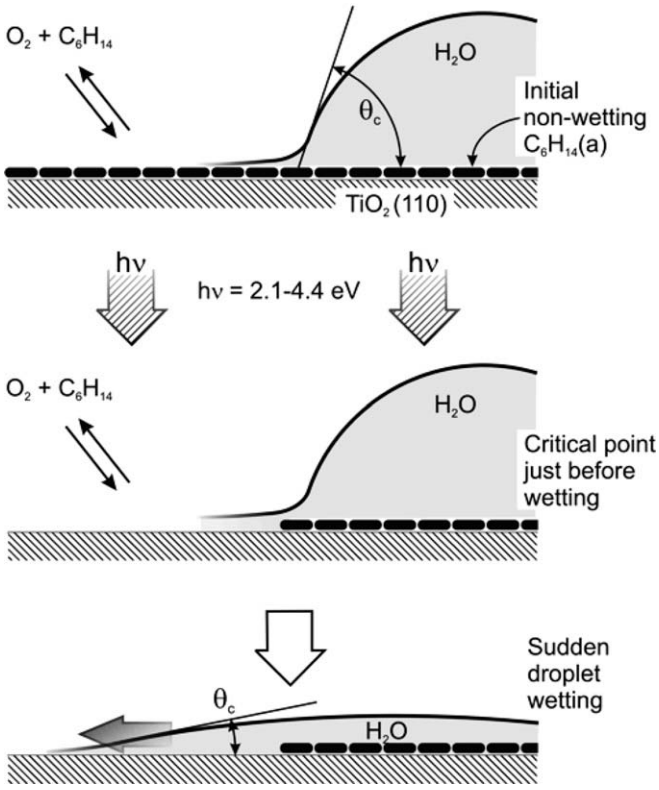

Fig. 15. Schematic interpretation of the sudden hydrophilic effect due to hydrocarbon photooxidation on TiO_2 (1 1 0) – 1 × 1. The contact angle is θ_c [27].

layer. This equilibrium is indicated by the double arrow. When photooxidation is initiated, the equilibrium is disturbed and the coverage of adsorbed hydrocarbon will slowly decrease in the region external to the droplet edge and eventually a critical hydrocarbon coverage, probably near zero, will be achieved, permitting the water droplet to suddenly wet the external surface. The hydrocarbon layer under the droplet is not photooxidized because the water bulk shields this surface from extensive exposure to O_2. In this experiment, estimates of the coverage of *n*-hexane in equilibrium with the atmosphere have been made based on the known

energetics of adsorption (Ref. [27], see Ref. [33] therein) and approximately 1 ML of adsorbed hexane will exist under the conditions of the experiment.

On the basis of these measurements of the photoinduced hydrophilicity effect on $TiO_2(110)-1\times1$, we conclude that the phenomenon is due to the removal by photooxidation of a monolayer adsorbed non-wetting hydrocarbon and that other models for this very important phenomenon are likely to be incorrect.

5. Summary and look to the future

This review has concerned two surface science studies from our own laboratory designed to reveal the underlying mechanisms of photochemistry on TiO_2 surfaces. Both studies employ careful control of surface conditions and care in experimental design. In the case of O_2 photodesorption from $TiO_2(110)$, the discovery of the dependence of the rate on the ½-power of the incident UV flux clearly shows that charge carrier recombination governs the efficiency and that methods to reduce recombination could therefore be effective in increasing the photochemical efficiency. In the case of the photoinduced hydrophilicity effect on TiO_2, it was shown that a simple model involving only the adsorbed hydrocarbon molecule coverage and its removal by photooxidation seems to govern the hydrophilicity phenomenon. This first observation of the sudden effect in wetting, and its implication on the origin of the photochemically induced hydrophilic phenomenon on TiO_2, provides new insight into the mechanism of this important new technological phenomenon. In both of these examples of photochemical studies carried out from the point of view of surface science, quantitative methods of measurement have been employed where attention to surface structure and cleanliness is centrally important. Indeed these methods are the hallmarks of the methods employed so successfully by Gerhard Ertl in his life's work!

Acknowledgements

I acknowledge, with thanks, the support of the Army Research Office for a DARPA-MURI grant as well as direct support for this work. I also thank Dr. Sunhee Kim for help with the figures and references in the article.

References

[1] G. Ertl, Angew. Chem. Int. Ed. 47 (2008) 3524.
[2] J.T. Yates Jr., H. Petek, Chem. Rev. 106 (2006) 4116.
[3] N.A. Tolk, M.M. Traum, J.C. Tully, T.E. Madey, in: Proceedings of Conference Series on Desorption Induced by Electronic Transitions, Springer Series in Chemical Physics, vol. 24, and succeeding DIET Conferences, 1983.
[4] R.D. Ramsier, J.T. Yates Jr., Surf. Sci. Rep. 12 (1991) 246;
X.L. Zhou, X.-Y. Zhu, J.M. White, Surf. Sci. Rep. 13 (1991) 73.
[5] A.L. Linsebigler, G. Lu, J.T. Yates Jr., Chem. Rev. 95 (1995) 735.
[6] T.L. Thompson, J.T. Yates Jr., Chem. Rev. 106 (2006) 4428.
[7] A. Fujishima, K. Honda, Nature 238 (1972) 37.
[8] M. Grätzel, Nature 414 (2001) 338.
[9] M. Grätzel, J. Photochem. Photobiol. C 4 (2003) 145.
[10] A. Hagfeldt, M. Graetzel, Chem. Rev. 95 (1995) 49.
[11] A. Fujishima, K. Hashimoto, T. Watanabe, TiO_2 Photocatalysis: Fundamentals and Applications, BKC, Inc., Tokyo, Japan, 1999.
[12] R. Wang, K. Hashimoto, A. Fujishima, M. Chikuni, E. Kojima, A. Kitamura, M. Shimohigoshi, T. Watanabe, Nature 388 (1997) 431;
R. Wang, K. Hashimoto, A. Fujishima, M. Chikuni, E. Kojima, A. Kitamura, M. Shimohigoshi, T. Watanabe, Adv. Mater. 10 (1998) 135.
[13] K. Sunada, Y. Kikuchi, K. Hashimoto, A. Fujishima, Environ. Sci. Technol. 32 (1998) 726.
[14] W. Shockley, W.T. Read Jr., Phys. Rev. 87 (1952) 835.
[15] T.L. Thompson, J.T. Yates Jr., J. Phys. Chem. B 110 (2006) 7431.
[16] G. Lu, A. Linsebigler, J.T. Yates Jr., J. Chem. Phys. 102 (1995) 4657.
[17] M.A. Henderson, W.S. Epling, C.L. Perkins, C.H.F. Peden, U. Diebold, J. Phys. Chem. B 103 (1999) 5328.
[18] C.N. Rusu, J.T. Yates Jr., Langmuir 13 (1997) 4311.
[19] M. Anpo, M. Che, B. Fubini, E. Garrone, E. Giamello, M.C. Paganini, Top. Catal. 8 (1999) 189.
[20] M.P. de Lara-Castells, J.L. Krause, J. Chem. Phys. 115 (2001) 4798.
[21] M.P. de Lara-Castells, J.L. Krause, Chem. Phys. Lett. 354 (2002) 483.
[22] T.L. Thompson, J.T. Yates Jr., J. Phys. Chem. B 109 (2005) 18230.
[23] T.L. Thompson, O. Diwald, J.T. Yates Jr., Chem. Phys. Lett. 393 (2004) 28.
[24] G. Lu, A. Linsebigler, J.T. Yates Jr., J. Chem. Phys. 102 (1995) 3005.
[25] C.J.G. Cornu, A.J. Colussi, M.R. Hoffmann, J. Phys. Chem. B 105 (2001) 1351.
[26] N. Sakai, A. Fujishima, T. Watanabe, K. Hashimoto, J. Phys. Chem. B 107 (2003) 1028.
[27] T. Zubkov, D. Stahl, T.L. Thompson, D. Panayotov, O. Diwald, J.T. Yates Jr., J. Phys. Chem. B 109 (2005) 15454.
[28] S. Mezhenny, P. Maksymovych, T.L. Thompson, O. Diwald, D. Stahl, S.D. Walck, J.T. Yates Jr., Chem. Phys. Lett. 369 (2003) 152.
[29] A. Bouzoubaa, A. Markovits, M. Calatayud, C. Minot, Surf. Sci. 583 (2005) 107.